Chapter 1

Graphene-Boron Nitride Composite: A Material with Advanced Functionalities

Sumanta Bhandary and Biplab Sanyal

Additional information is available at the end of the chapter

http://dx.doi.org/10.5772/50729

1. Introduction

The discovery of two dimensional materials is extremely exciting due to their unique properties, resulting from the lowering of dimensionality. Physics in 2D is quite rich (e.g., high temperature superconductivity, fractional quantum Hall effect etc.) and is different from its other dimensional counterparts. A 2D material acts as the bridge between bulk 3D systems and 0D quantum dots or 1D chain materials. This can well be the building block for materials with other dimensions. The discovery of graphene, the 2D allotrope of carbon by Geim and Novoselov [1] made an enormous sensation owing to a plethora of exciting properties. They were awarded the Nobel prize in Physics in 2010. Graphene, an atomically thick C layer, has broken the jinx of impossibility of the formation of a 2D structure at a finite temperature, as argued by Landau *et al.*[2, 3]. The argument that a 2D material is thermodynamically unstable due to the out-of-plane thermal distortion, which is comparable to its bond length, was proven invalid with this discovery. One of the recent interests is to understand this apparent discrepancy by considering rippled structures of graphene at finite temperatures.

Graphene, with its exciting appearance, has won the crowns of the thinnest, the strongest, the most stretchable material along with extremely high electron mobility and thermal conductivity [4]. The linear dispersion curve at the Dirac point gives rise to exciting elementary electronic properties. Electrons in graphene behave like massless Dirac fermions, similar to the relativistic particles in quantum electrodynamics and hence has brought different branches of science together under a truly interdisciplinary platform. At low temperature and high magnetic field, a fascinating phenomenon, called the half integer quantum hall effect, is observed. The relativistic nature of carriers in graphene shows 100% tunneling through a potential barrier by changing its chirality. The phenomenon is known as "Klein-Paradox". Minimum conductivity of a value of conductivity quantum (e^2/h per spin per valley) is measured at zero field, which makes graphene unique. "The CERN on table top" is thus a significant naming of the experiments performed with this fascinating material [5].

An infinite pristine graphene is a semi metal, i. e., a metal with zero band gap [6]. Inversion symmetry provided by $P6/mmm$ space group results in a band degeneracy at the Dirac points

(K and $K^{'}$) in the hexagonal Brillouin zone (BZ). This limits its most anticipated application in electronics as the on-off current ratio becomes too small to be employed in a device. The opening of a band gap is thus essential from electronics point of view retaining a high carrier mobility. Several approaches have been already made by modifying graphene, either chemically [7, 8] or by structural confinement [9–11] to improve its application possibilities, both from theory and experiment. It should be noted that in theoretical studies, the use of density functional theory (DFT) [12] has always played an instrumental role in understanding and predicting the properties of materials, often in a quantitative way.

Boron Nitride (BN), on the other hand, can have different forms of structures like bulk hexagonal BN with sp^2 bond, cubic BN with sp^3 bond, analogous to graphite and diamond respectively. A 2D sheet with strong sp^2 bonds can also be derived from it, which resembles its carbon counterpart, graphene. But two different chemical species in the two sublattices of BN forbid the inversion symmetry, which results in the degeneracy lifting at Dirac points in the BZ. Hexagonal BN sheet thus turns out to be an insulator with a band gap of 5.97 eV.

This opens up a possibility of alloying these neighboring elements in the periodic table to form another interesting class of materials. Possibilities are bright and so are the promises. B-N bond length is just 1.7% larger than the C-C bond, which makes them perfect for alloying with minimal internal stress. At the same time, introduction of BN in graphene, breaks the inversion symmetry, which can result in the opening up of a band gap in graphene. On top of that, the electronegativities of B, C, and N are respectively 2.0, 2.5 and 3.0 [13], which means that the charge transfer in different kinds of BCN structures is going to play an interesting role both in stability and electronic properties.

Hexagonal BNC (h-BNC) films have been recently synthesized [14] on a Cu substrate by thermal catalytic chemical vapor deposition method. For the synthesis, ammonia borane (NH_3-BH_3) and methane were used as precursors for BN and C respectively. In the experimental situation, it is possible to control the relative percentage of C and BN. The interesting point is that the h-BNC films can be lithographically patterned for fabrication of devices. The atomic force microscopy images indicated the formation of 2-3 layers of h-BNC. The structures and compositions of the films were characterized by atomic high resolution transmission electron microscopy and electron energy-loss spectroscopy. Electrical measurements in a four-probe device showed that the electrical conductivity of h-BNC ribbons increased with an increase in the percentage of graphene. The h-BNC field effect transistor showed ambipolar behavior similar to graphene but with reduced carrier mobility of 5-20 $cm^2V^{-1}s^{-1}$. From all these detailed analysis, one could conclude that in h-BNC films, hybridized h-BN and graphene domains were formed with unique electronic properties. Therefore, one can imagine the h-BN domains as extended impurities in the graphene lattice.

The structure and composition of BN-graphene composite are important issues to consider. As mentioned before, substitution of C in graphene by B and N can give an alloyed BCN configuration. Considering the possibilities of thermodynamic non-equilibrium at the time of growth process, one can think of several ways of alloying. The potential barrier among those individual structures can be quite high and that can keep these relatively high energetic structures stable at room temperature. For example, a huge potential barrier has to be crossed to reach a phase segregated alloy from a normal alloy, which makes normal alloy stable at room temperature. Now, depending on the growth process, different types of alloying are possible. Firstly, one can think of an even mixture of boron nitride and carbon, where one C_2

block is replaced by B-N. In this case, the formula unit will be BC_2N. Secondly, a whole area of graphene can be replaced by boron nitride, which makes them phase separated. This we call as phase segregated alloy. The formula unit of phase segregated alloy can change depending on the percentage of doping. The final part of the following section will be devoted to the phase segregated BCN alloys. Apart from those, a distributed alloying is possible with different BN:graphene ratios.

The substitution of C_2 with B-N introduces several interesting features. Firstly, B-N bond length is 1.7% bigger that C-C bond but C-B bond is 15% bigger than C-N bond. So, this is going to create intra-layer strain, which is going to affect its stability. Secondly, the difference in electro negativity in B (2.0) and N (3.0) will definitely cause a charge transfer. The orientation of charged pair B-N do have a major contribution in cohesive energy. Thirdly, as mentioned earlier, this will break inversion symmetry in graphene, which brings a significant change in electronic properties. Keeping these in mind, we are now going to discuss stability and electronic structure of BC_2N.

2. Stability of BC_2N

In this section we will mainly focus on the stability issues for various BC_2N structures [13, 15]. To demonstrate the factors for structural stability, we have chosen five different structures of BC_2N (Fig. 1). Let's first have a closer look at structure I. Every C atom has one C, N and B as nearest neighbors while B(N) has two Cs and one N(B) as their nearest neighbors. There is a possibility of all bonds to be relaxed, retaining the hexagonal structure. Stress is thus minimized in this structure, which helps obviously in the stability. In structure II, each C has two C and either one B or N as nearest neighbors. C_2 and BN form own striped regions, which lie parallel to each other in this structure. Now C-B bond is much larger that C-C. So this is definitely going to put some internal stress. From the point of view of intra-layer stress, this structure is definitely less stable than the previous one. Looking at structure III, one can see this structure looks similar to structure I but B-N bond orientations are different. Each C atom now has either two N or B and one C in its neighboring position while N(B) has two C and one B (N) as neighbors. This obviously adds some uncompensated strain in the structure. Structure III, thus consists of two parallel C-N and C-B chains and as C-B bond length is much larger than C-N (15%), this mismatch is going to introduce a large strain in the interface. On the other hand in structure I, C-N and C-B are lined up making the structural energy lower compared to structure III. Structure IV does not contain any C-C bond. C-B and C-N chains are lined parallel to each other. Finally in structure V, B-N bonds are placed in such a way that they make 60° angle to each other. Both of the last two structures thus have uncompensated strain, which increases their structural energies.

Bond energy is another key factor in stability. When the bond energies are counted, the ordering of the bonds is the following [13]:

$$B-N(4.00\,eV) > C-C(3.71\,eV) > N-C(2.83\,eV) > B-C(2.59\,eV) > B-B(2.32\,eV) > N-N(2.11\,eV)$$

The maximization of stable bonds like B-N and C-C will thus stabilize the structure as a whole. Now, a structure like II, with a striped pattern of C and B-N chains has maximum number of such bonds. This makes it most stable even though a structural strain is present. In this case bond energy wins over structural stress. For the structures like I and III, number

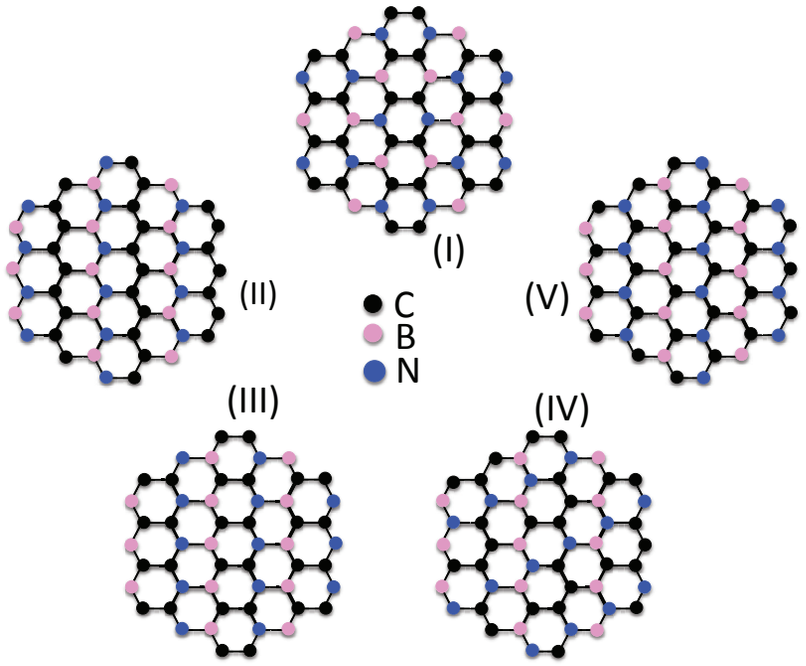

Figure 1. Crystal structure of different isomers of BC_2N. Filled black, pink, and blue circles represent carbon, boron and nitrogen respectively.

of such bonds is equal. In that case, intra-layer stress acts as the deciding factor. Structure IV, on the other hand does not have any C-C or B-N bond but only C-B or C-N. Therefore, the issue of stability is the most prominent here. The number of strong bonds is sufficiently large in structure V for the stabilization despite of 60° arrangement of B-N bonds.

Another important issue is the charge transfer as there is a difference between the electronegativities of B, C, and N. As mentioned earlier, N is the most electronegative and B is the least one while C behaves as a neutral atom. This also adds an ionic character in the bond formation. B (N) always gains some +ve (-ve) charges. So, the gain in the electrostatic energy only happens if these +/- charges are situated in an alternative manner. Otherwise the electrostatic repulsion makes the structure unstable. From this point of view, structures II, III, and V are more stable than the other two following the trend shown from bond energies. Thus, as reported by Itoh *et al.*[13], ordering of the structures will be: II>V>(I,III)>IV . Stability of other possible isomers can as well be anticipated with the same arguments.

So far we have talked about the substitutional alloying of BN and graphene, where BN to C_2 ratio is 1:1. Another group of structures, which can be formed by alloying BN and graphene is the phase segregated BCN. In this kind of structure, BN (graphene) retains its own phase, separated by graphene (BN). The experimental evidence of these kinds of structures have been shown [14]. The size of the graphene or BN phase has an impact on the stability and electronic properties. Here, the BN:C_2 ratio is thus not only 1:1 but can be varied and if varied controllably, one can control the electronic properties such as band gap [16]. Lam *et al.*[16] have shown that, by controlling the graphene phase, one can control the band gap according to the desired values for technological applications. The phase segregated $(BN)_m(C_2)_n$ alloys

are also found to be stable over the first kind of alloying, which indicates a transformation due to thermal vibration. Yuge *et al.*[17] with DFT studies and Monte Carlo simulations have shown a tendency of phase separation between BN and graphene.

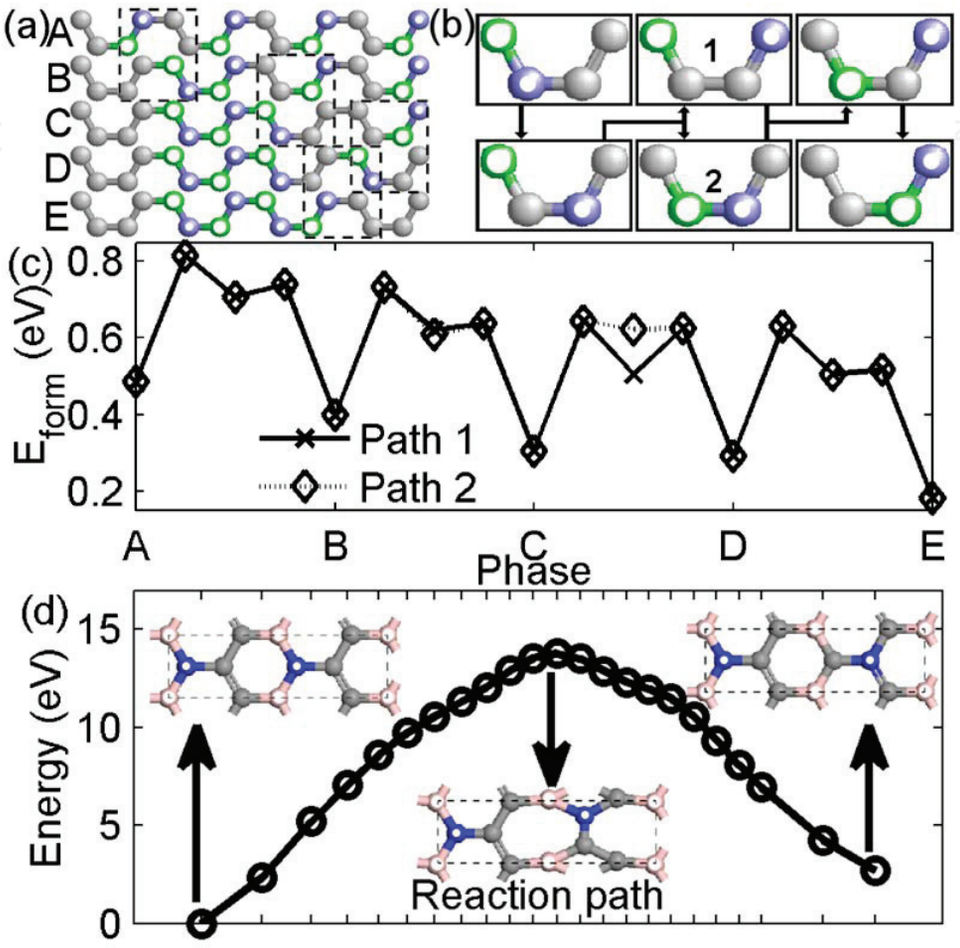

Figure 2. (a) Different steps (A-E) of phase separation process, (b) Swapping of BN and C dimers, (c) Formation energies for different steps shown in (a) for two different paths demonstrated in (b), (d) Activation energy in going from left to right configuration in the initial step of phase segregation. Reprinted with permission from Appl. Phys. Lett. 98, 022101 (2011). Copyright (2011) American Institute of Physics.

Even though a tendency is indicated, a recent calculation by Lam *et al.*, have shown that this possibility is hindered as the activation energy required for phase segregation is extremely high. As shown in Fig. 2, they have chosen a possible path for phase separation by swapping B-N bond to C-C bonds. This kind of swapping can also happen in two ways (Fig. 2(b)). Calculated formation energies for these two process are shown in Fig. 2(c), which basically demonstrates that the intermediate structures are quite high in energy compared to evenly distributed and phase separated structures. The authors also performed nudged elastic band (NEB) calculations to determine the activation barriers for the first step to occur, i. e. to change a B-N bond to B-C and N-C bonds (Fig. 2(d)). Activation energy required is 1.63eV/atom suggesting that this process can happen only at elevated temperatures. At room temperature that is why the pristine $(BN)_m(C_2)_n$ should be stable and so are the phase separated ones.

There can be two different patterns for phase segregated BCN alloys. One is the phase separated island-like and the other one is a striped pattern. The island-like pattern consists of larger graphene-BN interface region than that in the striped pattern. This means that the number of B-C and N-C bonds are less in striped pattern than in an island form. As we have discussed earlier, the maximization of C-C and B-N bonds thus favors a striped pattern [13].

Till now, we have discussed mainly the stability issues of $(BN)_m(C_2)_n$ with 1:1 ratio and phase separated BCN alloys. A distributed mixture of BN and graphene with different $m : n$ ratios can also form depending on the growth condition. Different isomeric structures are also possible for a particular $m : n$ ratio. In the following section we are going to present a DFT study to analyze the stability and electronic properties of $(BN)_m(C_2)_n$ with different $m : n$ ratios. Utilizing the concept of aromaticity, the aim is to find out stable isomers for a particular $m : n$ ratio and also to explore the possibilities of achieving desired electronic properties.

Aromaticity, as extensively used to determine the stability of organic molecules, can provide us a working principle for determining stability of the structures as well. Benzene (C_6H_6) is the prototype for the organic molecules, which are stabilized by aromaticity. Borazine ($B_3N_3H_6$), an isoelectric BN analogue of benzene on the other hand has one-third stability of benzene from the point of view of aromaticity [18–21]. This is particularly interesting in $(BN)_m(C_2)_n$, as the admixture of two not only changes the electronic property but also affects its stability. To investigate a stable isomer, our first working principle thus is to maximize the carbon hexagons, which essentially mimic benzene rings. A carbon-hexagon again can be surrounded by BN and each hexagon can be kept aloof or all hexagons can form a carbon-pathway. In a carbon pathway, π-conjugation is allowed whereas it is hindered in isolated C-hexagons.

To look for reasonable isomers, we consider that the following structural possibilities will not occur. Firstly, a hexagon will not contain B and N in 1 and 3 positions with respect to each other. These kind of structures are described by zwitterionic and biradical resonance structures, which basically result in an odd number of π-electrons on two of the Cs in the hexagon (Fig. 3).

Hence, a B-N pair should be placed either in 1,4 or 1,2 position in the hexagon with respect to each other. π-electrons will thus be distributed over a C-C bond and form a resonance structure. Second kind of structural constraint, that we consider, is the absence of B-B or N-N bonds. As discussed earlier, these kind of bonds result in the lowering of π-bonds and thus decreased relative stability of an isomer.

The relative positions of B and N around an all C hexagon is also a key factor that controls the electronic properties. To illustrate the phenomenon, let's consider the following two isomers. As in Fig. 3, the isomer I and isomer II, both have similar chemical configuration. But in Isomer I, B and N are connected to C at position 1 and 4 in the hexagon, which we can call B-ring-N para-arrangement. A donor- acceptor (D-A) interaction is thus established in this kind of structural arrangement. On the other hand in isomer II, B and N are connected to 1^{st} & 2^{nd} (4^{th} & 5^{th}) positioned C atoms in the hexagon. Although a D-A interaction occurs between neighboring B and N, B-ring-N interaction is forbidden. The local D-A interaction around a C-hexagon, as shown in Fig. 4, increases the HOMO-LUMO gap whereas N-ring-N (or B-ring-B) para arrangement results in the lowering of the HOMO-LUMO gap.

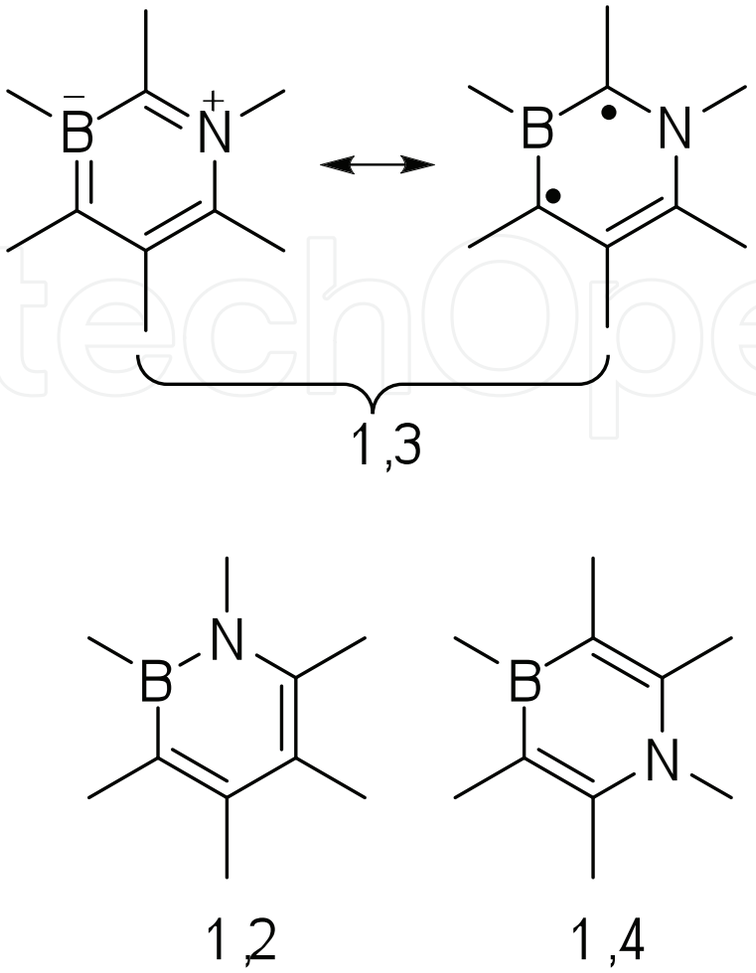

Figure 3. Schematic representation of zwitterionic and biradical resonance structures. Reprinted with permission from J. Phys. Chem. C 115, 10264 (2011). Copyright (2011) American Chemical Society.

We have performed density functional calculations to investigate the isomers of $(BN)_m(C_2)_n$ [22]. All the structures are optimized with both (Perdew-Burke-Ernzerhof) PBE [23] and (Heyd-Scuseria-Ernzerhof) HSE [24] functionals. The functionals based on local spin density approximation or generalized gradient approximations reproduce the structural parameters reasonably well, whereas the band gaps come out to be much smaller compared to experiments. The reason behind this is the self interaction error. HSE, with a better description of exchange and correlation within hybrid DFT, yields a band gap, which is much closer to the experimental value.

The degree of aromaticity is calculated quantitatively, with a harmonic oscillator model of aromaticity (HOMA) prescribed by Krygowski *et al.*[25]. The HOMA value of an ideal aromatic compound (Benzene) will be 1, whereas the value will be close to zero for non aromatic compounds. Anti-aromatic compound with the least stability will have a negative HOMA value. As mentioned earlier, the aim is to find the important isomers with relatively high stability and reasonable band gaps among $(BN)_m(C_2)_n$ compounds with $m : n$ ratios 1:1, 2:1, 1:3 and 2:3. Let's focus on each type separately.

2.1. 1:1 h-BN:Graphene (BC_2N)

We have considered six isomers for BC_2N, among which two structures BC_2N-I and BC_2N-II consist of all C-hexagon pathways. In the third one,BC_2N-III, all C-hexagons are connected linearly as in polyacenes where as the fourth one , BC_2N-IV, has disconnected all-C-hexagons. The other two structures, BC_2N-V & BC_2N-VI do not have any all-C hexagon but BC_2N-VI has at least polyacetylene paths whereas BC_2N-V has only isolated C-C bonds. Although there

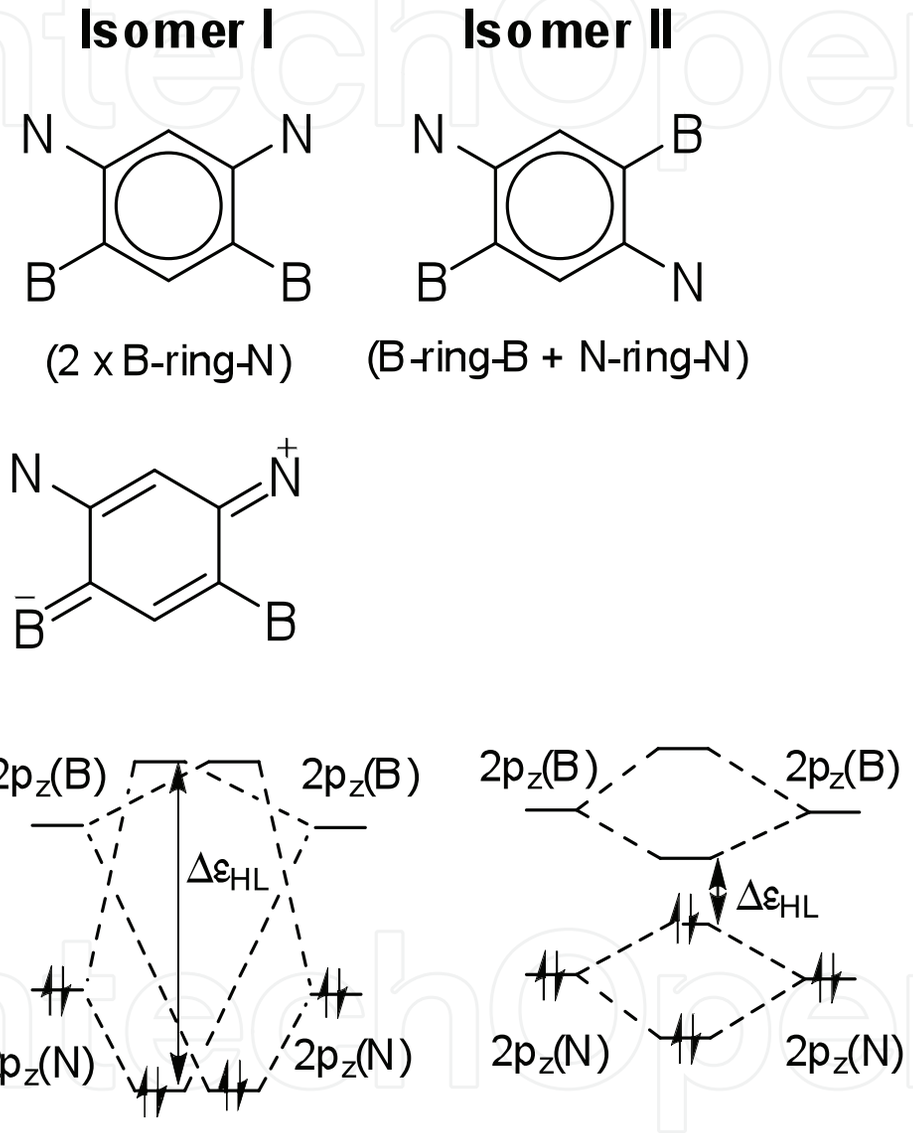

Figure 4. Qualitative representation of opening up a band gap and D-A interaction in isomer I and reduction of band gap in isomer II, with molecular orbital diagrams and valence bond representation. Reprinted with permission from J. Phys. Chem. C 115, 10264 (2011). Copyright (2011) American Chemical Society.

are several other isomers possible, we limit ourselves with these and try to understand the properties with the knowledge of aromaticity and conjugation. Firstly, the first three isomers, among all six are most stable and the relative energies differ by at most 0.15 eV (PBE) and 0.07 eV (HSE). The presence of all C-hexagons connected to each other not only increases the

stable C-C and B-N bonds but also helps in the π-conjugation. The result is reflected in the HOMA values of first two structures, which are 0.842 and 0.888 respectively. This suggests the formation of aromatic benzene like all-C hexagons. The HOMA value of BC_2N-III is little less (0.642) but this structure in particular is not stable due to aromaticity rather due to the formation of polyacetylene paths. A slightly lower HOMA value observed in BC_2N-I compared to BC_2N-II is due to the difference in B-C bond (0.02Å), which leads to a change in D-A interaction.

If we look at the formation energies of BC_2N-IV & BC_2N-VI, the values are quite close. BC_2N-IV consists of completely isolated all-C hexagons. This is the reason of having high aromaticity of 0.88. But at the same time this increases N-C & B-C bonds and restricts π-conjugation. Therefore, this structure is less probable thermodynamically. BC_2N-VI, which was suggested to be the most stable BC_2N structure by Liu *et al.*[15], on the other hand has no aromatic all C-hexagon. But this structure contains all-C polyacetylene paths with C-C bond length 1.42 Å, which explains its low formation energy. BC_2N-V is the least stable among all, which has neither all-C hexagon nor polyacetylene C-paths. Obviously most unstable B-C and B-N bonds are maximized here creating an enormous strain in the structure. The presence of only C-C bond of 1.327 Å explains that. These factors make this compound thermodynamically most unstable among all five structures.

All these results give us a stand point from where we can judge the thermodynamic stability of other $(BN)_m(C_2)_n$ structures with the following working principles in hand:

(a) π-Conjugation within all C path increases stability.

(b) The formation of aromatic all C-hexagons also does the same, while this is more effective when hexagons are connected.

(c) There is not much contribution of B-ring-B or B-ring-N arrangement of B and N around poly(para-phenylene) (PPP) path in total energies. But indeed these, as discussed earlier, will affect the band gap, which we will present in the following section.

Coming to the band gap issue, the first three structures, which are close in energy, have band gaps ranging from 1.6 to 2.3 eV in HSE calculations (0.7 to 1.7 eV in PBE). The difference in BC_2N-I & BC_2N-II comes from the arrangement of B and N around all-C hexagon. As discussed in Fig. 3, D-A interaction increases for para-positions (i. e.1,4 or 2,6), which is observed in BC_2N-I. The band gap is 0.5 eV (0.65 eV in PBE), higher than that in BC_2N-II, where B and N are oriented in ortho-position (i. e.1,2 or 4,5). Quite obviously, BC_2N-III has all-C chain, which resembles a graphene nanoribbon and has the least value of the band gap.

2.2. 2:1 h-BN:Graphene (BCN)

We have investigated three structures of BCN, which have recently been synthesized [26]. The first one (BCN-I) has aromatic all-C hexagons connected in PPP path whereas the second one (BCN-III) contains all-C hexagon but connected in zigzag polyacene bonds. The final one (BCN-IV) consists of neither all-C hexagon nor a stripe of all-C region. BCN-I & BCN-II are iso-energetic, which is expected and is $\sim$ 0.5 eV lower than BCN-IV. This again explains the importance of aromatic all-C hexagon and π-conjugation. The absence of these and also the increased B-C, N-C bonds make BCN-IV relatively unstable. Another key point in BCN-I & BCN-I is the position of B and N around the hexagon. The stability may not be affected but

the band gap is definitely changed by this. As expected, from the discussion in Fig. 4, BCN-I has a quite high value of the band gap. Aromaticity is higher in BCN-I (0.846) compared to BCN-III (0.557) , which is also seen in BC_2N structures. Iso-energetic BCN-I & BCN-II are equally probable during growth process but with a band gap range 1.3 to 2.7 eV .

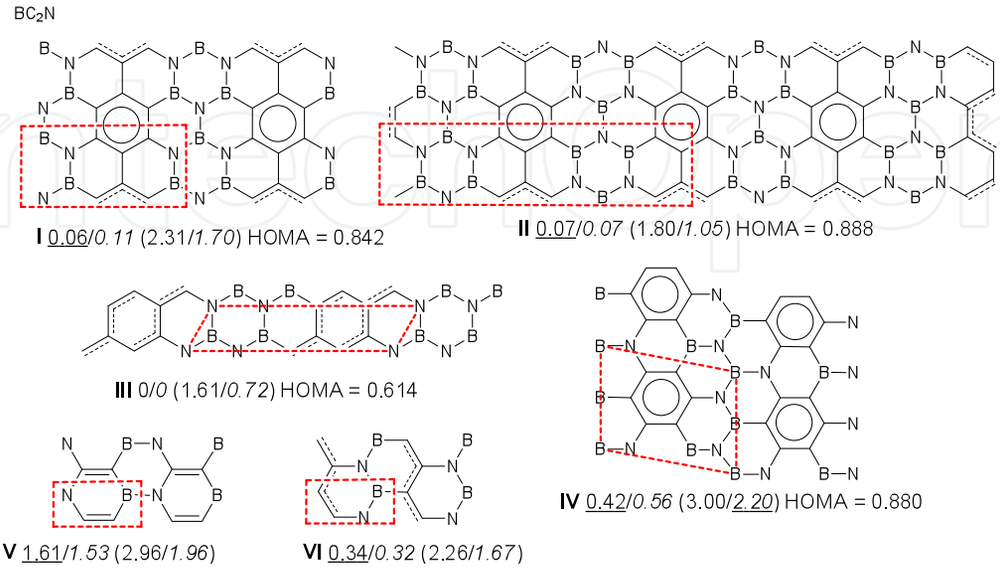

Figure 5. Six isomers of BC_2N are considered for this study. Relative energy (per formula unit) with respect to most stable structures and band gaps (in parentheses) are shown from HSE (normal print) and PBE (italic) calculations. HOMA values of all-C hexagons, obtained from HSE calculations are also provided. Reprinted with permission from J. Phys. Chem. C 115, 10264 (2011). Copyright (2011) American Chemical Society.

2.3. 2:3 & 1:3 h-BN:Graphene (BC_3N & BC_6N)

We now gradually increase the C-percentage with the anticipation of lowering the band gap because of increased graphene region. Two structures of BC_3N and three structures of BC_6N have been examined. Both the structures of BC_3N consist of aromatic hexagonal all-C rings connected in PPP path. The similarity in HOMA values depicts that picture. The position of B and N around C-ring is different though in BC_3N-I and BC_3N-II. The para arrangement of B-ring-N results in a large band gap in BC_3N-I (2.14 eV) while the ortho arrangement of the same in BC_3N-II lowers the value of the band gap. The stability is not affected by that fact as aromaticity and π-band formation are quite similar, which make those structures iso-energetic. A similar situation is also seen in BC_6N structures. BC_6N-I and BC_6N-II are iso-energetic mainly due to a similarity in structures. Both of them contain all-C rings connected in PPP path. But in the third one (BC_6N-III), all-C rings are separated, which makes this structure relatively unstable due to restricted π-conjugation. The HOMA value is maximum (0.93) in BC_6N-III, whereas the values are 0.78 and 0.86 respectively for BC_6N-I and BC_6N-II. The para arrangement of B-ring-N in BC_6N-I and BC_6N-III leads to large band gaps (1.58 and 1.34 eV respectively) while ortho-positioning of the same results in a reduced band gap in BC_6N-II. Finally, we have summarized the calculated (HSE and PBE) band gaps for all $(BN)_m(C_2)_n$ isomers (Fig. 7A and Fig. 7B). As expected, the band gaps are increased for HSE functional. Apart from that, both HSE and PBE -level calculations show a similar trend. A

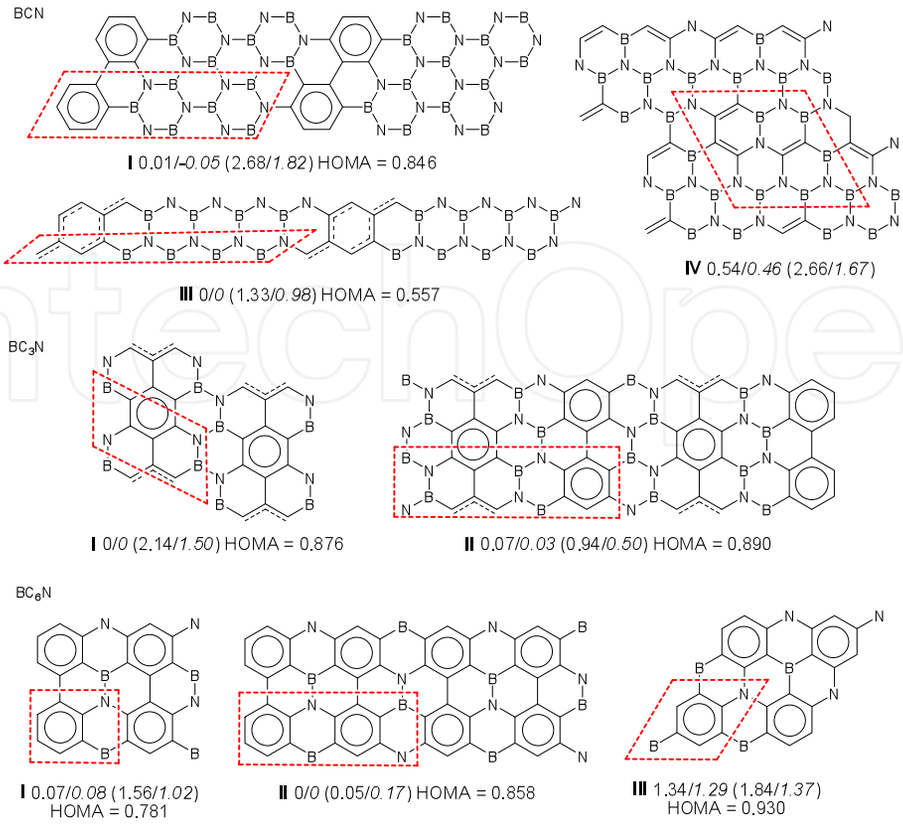

Figure 6. The isomers of BCN, BC_3N, BC_6N. Relative energy (per formula unit) with respect to most stable structures and band gaps (in parentheses) are shown from HSE (normal print) and PBE (italic) calculations. HOMA values of all-C hexagons, obtained from HSE calculations are also provided. Reprinted with permission from J. Phys. Chem. C 115, 10264 (2011). Copyright (2011) American Chemical Society.

general trend is observed that an increase in the graphene region reduces the band gap. All the lowest energy structures for different compositions of $(BN)_m(C_2)_n$ have band gaps around 1 eV, which is a desired value for technological applications. One very important thing that we learnt from this study is that the position of B and N around C-ring controls the band gap without affecting the stability.

3. Functionalization

Incorporation of magnetism in 2D sp-materials has been an important point of discussion in recent times. The combination of localized moments of 3*d* transition metal atoms and the *sp* electrons of the host 2D lattice can give rise to interesting magnetic properties relevant to nano devices based on the principle of magnetoresistance, for example. Ferromagnetic long-ranged order, half metallicity, large magnetic anisotropy, electric field driven switching of magnetization etc. are being studied for transition metal atoms adsorbed on graphene and 2D BN sheets. Another important point is the adsorption of these species at the interface between BN and graphene. A recent study [27] based on first principles electronic structure calculations has revealed some interesting electronic and magnetic properties of Fe, Co and Ni adatoms adsorbed on a h-BC_2N sheet. A hexagonal site at the interface between BN and graphene

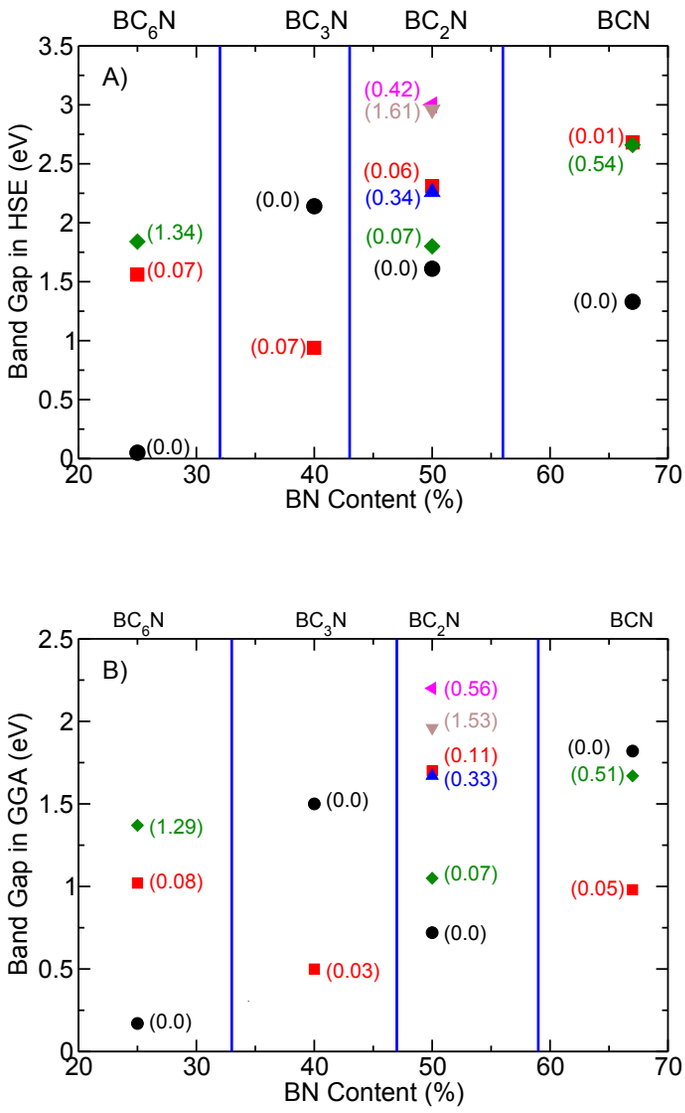

Figure 7. Band gaps of different isomers of $(BN)_m(C_2)_n$ are plotted against BN density, obtained from both (A) HSE and (B) PBE calculations. Relative energies are given in parentheses.

turns out to be a favorable site for adsorption. The presence of Fe, Co and Ni makes the system a magnetic semiconductor, a magnetic semi-metal and a non magnetic semiconductor respectively. Another interesting observation was that the adatoms are highly mobile on the surface and hence have the possibility to have a clustered configuration among themselves. It is interesting to note that the properties of this hybrid system are tunable in the sense that they can be modified by having different combinations of the width of each subsystem, BN and graphene.

Not only by magnetic adatoms, but by intrinsic edge properties, one can render magnetism in these 2D sheets. By DFT calculations, Dutta *et al.* [28] predicted interesting magnetic properties of H-passivated zigzag nanoribbons (ZGNRs) of various widths, doped by boron and nitrogen, keeping the whole system isoelectronic with C atoms in graphene. In the

extreme case, all C atoms of ZGNRs are replaced by B and N atoms and zigzag BN nanoribbons are formed. In the ground state, the two edges are antiferromagnetically coupled and remain so for all dopings. However, the application of an external electric field affects the electronic structure of the nanoribbon giving rise to semiconducting and half-metallic properties. Electric-field induced changes in the magnetic properties are very interesting from a technological point of view. Other related studies [29] based on DFT revealed energetics, electronic structure and magnetism of quantum dots and nanorods of graphene embedded in BN sheet. It was showed that the formation energies and the HOMO-LUMO gaps of quantum dots vary as $1/\sqrt{n}$, where n is the number of carbon atoms in the dots.

Adsorption of gases on 2D materials is an important topic from the technological and environmental points of view. Materials for clean energy are always sought for and in this respect, efficient hydrogen uptake of suitable materials is an important issue. Raidongia *et al.* [26] have studied H_2 adsorption on BCN at 77 K and 1 atm. pressure. From their experiments, H_2 uptake of 2.6 wt % was observed. Also, CO_2 adsorption is very important for environmental issues. In their study, BCN was found to have a very high CO_2 uptake of 100 wt % at 195 K and 1 atm. pressure. It should be noted that the uptake is only 58 % by the activated charcoal under identical conditions. At room temperature and 40 bar pressure, the CO_2 uptake was found to be 44 wt %.

In a recent theoretical study, Cao *et al.* [30] showed that a zigzag interface between BN and graphene can have a strong capability of adsorbing hydrogen, much stronger than pure graphene, BN or the armchair interface between them. Moreover, the adsorption of hydrogen induces a semiconductor to metal transition. As the mobility of hydrogen on the surface is rather high, the hydrogen atoms can migrate to the zigzag interface and hence will increase the density of hydrogen storage with the added functionality of band gap engineering.

4. Summary and outlook

Graphene-BN nanocomposites offer a huge potential in various technological sectors, e.g., nano electronics, gas sensing, hydrogen storage, nanomagnetic storage devices, to name a few. The unique combination of these two materials with different electronic properties, forming a 2D network, offers many possibilities for studying fundamental science and applications for nanotechnology. However, many challenges, both in the domains of experiment and theory, will come in the way. Experimental synthesis of samples of good quality and state-of-the-art characterization techniques to reveal the atomic scale physics will be the issues. From the point of view of theory, one faces difficulties in having a correct description of the band gaps and electronic structures in standard approximations of materials-specific theories. However, with the availability of powerful supercomputing facilities, it is nowadays possible to treat large systems by sophisticated many body theories to have a much better quantitative descriptions. Nevertheless, one may envisage many interesting directions for the applications of these nanocomposites to utilize the interface properties of BN and graphene. One of them is the spin switching properties of organometallics adsorbed at the interface, similar to what has been studied recently [31] for a 2D graphene sheet. The other application can be the adsorption of amino acids [32] at the interface to increase the activity by their immobilization. Hopefully, in near future, we will observe many applications of these nanocomposites, useful for the human society.

Author details

Sumanta Bhandary and Biplab Sanyal
Department of Physics and Astronomy, Uppsala University, Box 516, 751 20 Uppsala, Sweden

5. References

[1] K. S. Novoselov, A. K. Geim, S. V. Morozov, D. Jiang, Y. Zhang, S. V. Dubonos, I. V. Grigorieva, A. A. Firsov, *Science* 306, 666 (2004).
[2] L. D. Landau, Phys. Z. Sowjetunion 11, 26 (1937).
[3] R. E. Peierls, Ann. I. H. Poincare 5, 177 (1935).
[4] A.K. Geim and K.S. Novoselov, Nat. Mater. 6, 183 (2007); A.H. Castro Neto *et al.*, Rev. Mod. Phys. 81, 109 (2009); A.K. Geim, Science 324, 1530 (2009).
[5] M. I. Katsnelson, Materials Today 10, 20 (2007).
[6] P. R. Wallace, Phys. Rev. 71 622-634 (1947).
[7] J. O. Sofo, A. S. Chaudhari and G. D. Barber, Phys. Rev. B 75, 153401 (2007); D. C. Elias *et al.*, 323, 610 (2009); O. Leenaerts, H. Peelaers, A. D. HernĞndez-Nieves, B. Partoens, and F. M. Peeters, Phys. Rev. B 82, 195436 (2010).
[8] M. Klintenberg, S. Lebegue, M. I. Katsnelson, and O. Eriksson, Phys. Rev. B 81, 085433(2010).
[9] M. Y. Han, B. Özyilmaz, Y. Zhang, and P. Kim, Phys. Rev. Lett. 98, 206805 (2007).
[10] Y.-W. Son, M. L. Cohen and S. G. Louie, Nature 444, 347 (2006).
[11] S. Bhandary, O. Eriksson, B. Sanyal and M I. Katsnelson, Phys. Rev. B 82,165405 (2010).
[12] P. Hohenberg and W. Kohn, Phys. Rev. B 136, 864 (1964); W. Kohn and L. J. Sham, Phys. Rev. A 140, 1133 (1965).
[13] H. Nozaki and S. Itoh, J. Phys. Chem. Solids, 57, 41 (1996).
[14] L. Ci, L. Song, C. Jin, D. Jariwala, D. Wu, Y. Li, A. Srivastava, Z. F. Wang, K. Storr, L. Balicas, F. Liu and P. M. Ajayan, Nat. Mater. 9, 430 (2010).
[15] A. Y. Liu, R. M. Wentzcovitch and M. L. Cohen, Phys. Rev. B 39,1760 (1989).
[16] K.-T. Lam, Y. Lu, Y. P. Feng and G. Liang, Appl. Phys. Lett. 98, 022101 (2011).
[17] K. Yuge, Phys. Rev. B 79, 144109 (2009).
[18] P. v. R. Schleyer, H. Jiao, Pure Appl. Chem 68, 209 (1996).
[19] E. D. Jemmis and B. Kiran, Inorg. Chem. 37, 2110 (1998).
[20] P. W. Fowler and E. J. Steiner, J. Phys. Chem. A 101, 1409 (1997).
[21] W. H. Fink, J. C. Richards, J. Am. Chem. Soc. 113, 3393 (1991).
[22] J. Zhu, S. Bhandary, B. Sanyal and H. Ottosson, J. Phys. Chem. C 115, 10264 (2011).
[23] J. P. Perdew and Y. Wang, Phys. Rev. B 45, 13244 (1992).
[24] J. Heyd and G. E. Scuseria, J. Chem. Phys. 120, 7274 (2004); J. Heyd, G. E. Scuseria and M. Ernzerhof, J. Chem. Phys. 118, 8207 (2003).
[25] T. M. Krygowsky, J. Chem. Inf. Comput. Sci. 33, 70 (1993).
[26] K. Raidongia, A. Nag, K. P. S. S. Hembram, U. V. Waghmare, R. Datta and C. N. R. Rao, Chem. Eur. J. 16, 149 (2010).
[27] P. Srivastava, M. Deshpande and P. Sen, Phys. Chem. Chem. Phys. 13, 21593 (2011).
[28] S. Dutta, A. K. Manna and S. K. Pati, Phys. Rev. Lett. 102, 096601 (2009).
[29] S. Bhowmick, A. K. Singh and B. I. Yakobson, J. Phys. Chem. C 115, 9889 (2011).
[30] T. Cao, J. Feng and E. G. Wang, Phys. Rev. B 84, 205447 (2011).
[31] S. Bhandary, S. Ghosh, H. Herper, H. Wende, O. Eriksson and B. Sanyal, Phys. Rev. Lett. 107, 257202 (2011).
[32] S. Mukhopadhyay, R. H. Scheicher, R. Pandey and S. P. Karna, J. Phys. Chem. Lett. 2, 2442 (2011).